Effect of Surface Asperity Truncation on Thermal Contact Conductance

Fernando H. Milanez, M. Michael Yovanovich, and J. Richard Culham, *Member, IEEE*

***Abstract*—This paper presents studies on thermal contact conductance at light contact loads. Surface profilometry measurements are presented which show that actual surface asperity height distributions are not perfectly Gaussian. The highest asperities are truncated, causing existing thermal contact conductance models to underpredict experimental data. These observations have been incorporated into modifications of existing contact conductance models. The truncation leads to an enhancement of thermal contact conductance at light contact pressures. The preliminary model has been compared against thermal contact conductance data presented in the open literature, and good agreement is observed. The results show that the truncation is a function of the roughness level: the rougher the surface, the more truncated the surface height distribution.**

***Index Terms*—Bead blasted surfaces, light contact pressures, mean separation gap, truncated Gaussian model.**

NOMENCLATURE

A	Contact area, m^2.
a	Mean contact spot radius, semi-major elliptic contact spot axis, m.
b	Semi-minor elliptic contact spot axis, m.
C_c	Dimensionless contact conductance [see (17)].
c_1	Vickers microhardness correlation coefficient, Pa.
c_2	Vickers microhardness correlation coefficient.
E	Young's modulus, Pa.
E'	Equivalent Young's modulus, Pa, [see (4)].
H_c	Plastic contact hardness, Pa.
h_c	Contact conductance, W/m^2 K.
k_s	Harmonic mean thermal conductivity, W/mK. $= 2k_Ak_B/(k_A + k_B)$.
m	Mean absolute roughness profile slope.
Nb	Niobium.
Ni	Nickel.
n	Density of contact spots, m^{-2}.
P	Apparent contact pressure, Pa.
p	Probability density function.
SS	Stainless Steel.
v	Minimum to maximum slope ratio, $(=m_{mn}/m_{mx})$.
Y	Mean separation gap, m.
z	Surface height, m.
Zr	Zirconium.

Greek Symbols

ϕ	Thermal constriction factor.
λ	Dimensionless mean separation gap, m, $(=Y/\sigma)$.
ν	Poisson's ratio.
σ	RMS of surface roughness, m.

Subscripts

A, B	Contacting bodies.
a	Apparent.
r	Real.
mn	Minimum.
mx	Maximum.
$trunc$	Truncation.
TG	Truncated Gaussian model.

I. INTRODUCTION

SINCE actual surfaces present deviations from their idealized geometrical form, known as roughness and waviness, when two solids are put into contact they will touch only at their highest asperities. Roughness is a small scale or short wavelength imperfection while waviness is a large-scale or long wavelength imperfection. The heat transfer across the interface of real solids is not as effective as if the solids were perfectly smooth and flat. A resistance to heat flow, known as thermal contact resistance, appears at the interface between solids. Heat transfer across the interface between two solids has been the subject of study by various researchers over many years. Contact heat transfer has many applications in engineering, such as ball bearings, microelectronic chips and nuclear fuel elements. In some circumstances, the contact pressure in these applications may be relatively low, such as when clamping devices are used in microelectronics applications or when one is interested in what happens to contact conductance if the contact pressure between the nuclear fuel and the nuclear fuel sheath drops bellow expected.

When two solids are pressed together, the contacting asperities will deform and form small spots of solid-solid contact. In the remaining portion of the apparent contact area the bodies are separated by very thin gaps. Heat transfer between two contacting solids can take place by three different modes: conduction through the contact spots, radiation through the gap in the remaining part of the apparent area and conduction through the gas that fills the gap. Radiation is important only at high temperatures, gap conductance can be neglected in vacuum applications, while contact conductance is always important. These

Manuscript received December 1, 2002; revised January 10, 2003. This work was supported by the Brazilian Federal Agency for Post-Graduate Education-CAPES and the Natural Sciences and Engineering Research Council of Canada. This work was recommended for publication by Associate Editor K. Ramakrishna upon evaluation of the reviewers' comments.

The authors are with the Microelectronics Heat Transfer Laboratory, Department of Mechanical Engineering, University of Waterloo, Waterloo, ON N2L 3G1, Canada (e-mail: milanez@mhtlab.uwaterloo.ca; mmyov@mhtlab.uwaterloo.ca; rix@mhtlab.uwaterloo.ca).

Digital Object Identifier 10.1109/TCAPT.2003.811469

three heat transfer modes are treated separately and the sum of the conductances associated with each of these heat transfer modes is called joint conductance.

This work is focused on the contact conductance, which is due to conduction through the contact spots. A thermal contact conductance model is generally composed of three models: thermal, geometrical and mechanical deformation models. The thermal model predicts the contact conductance for a given set of contact parameters: shape, size and distribution of contact spots. These contact parameters are obtained from a particular mechanical deformation model, which can be elastic, plastic or elastoplastic. The deformation model requires a geometric model of the surface in order to be able to predict the contact parameters.

Since it is extremely difficult to predict or to characterize the geometry of actual surfaces by deterministic means, statistical analysis has been generally employed. It is commonly assumed that the surface heights of actual surfaces follow the Gaussian distribution. The Gaussian height distribution model has been used in several thermal contact conductance models, such as the Cooper *et al.* [1] and the Greenwood and Williamson [2] models, as well as a number of other models derived from these two. It has been reported in the literature [3]–[7] that these thermal contact models tend to underpredict experimental data at light contact pressures, and as the pressure increases the models and measurements agree. The light contact pressure range is when the ratio between the apparent contact pressure P and the plastic hardness of the material H_c is $P/H_c < 5 \cdot 10^{-4}$, approximately. The cause of this behavior was unclear up to now and this subject is addressed here. This work presents evidence that the cause for the models to underpredict the experimental data at light contact pressures is the truncation of the highest asperities. The Gaussian model fails to predict accurately the contact parameters at light contact pressures. A new surface geometric model, called Truncated Gaussian, is proposed here. Modifications are incorporated to the well-established thermal contact conductance models in order to take into account the truncation of the height distribution of actual surfaces. The new thermal contact conductance model explains very well why the existing models underpredict the data at low loads while they are accurate at higher contact pressures, as it will be seen.

The next section provides a review of some of the thermal contact conductance models available in the literature. After that, the asperity truncation problem is identified and the new models are presented. The new models are compared against experimental data available in the literature.

II. Review of Existing Models

Most of the thermal contact conductance models available in the literature employ the same thermal model. Cooper *et al.* [1] first presented the solution for the thermal part of the contact conductance problem. They developed a thermal model for the contact between conforming isotropic rough surfaces, such as those obtained by lapping and bead blasting. The contact between surfaces possessing these features generates approximate circular contact spots randomly distributed over the apparent contact area. The thermal contact conductance between conforming isotropic rough surfaces is given by [1], [8]

$$h_c = \frac{2k_s n a}{\left(1 - \sqrt{A_r/A_a}\right)^{1.5}} \tag{1}$$

where n is the density of contact spots per unit apparent area, a is the mean contact spot radius and A_r/A_a is the real-to-apparent contact area ratio. The term in the denominator of the expression above is called the thermal constriction factor and takes into account for the constriction resistance of the heat flow near the contacting spots. DeVaal [7] extended the Cooper *et al.* [1] isotropic model to the contact between anisotropic surfaces, such as those obtained by grinding. The contact between such surfaces present elliptical spots rather than circular. The thermal contact conductance between conforming anisotropic rough surfaces is given by

$$h_c = \frac{k_s n \sqrt{\pi\, a\, b}}{2\,\phi\,(v,\, A_r/A_a)} \tag{2}$$

where a and b are, respectively, the mean semi-major and semi-minor axis of the elliptic contact spots, ϕ is the thermal constriction factor and v is the ratio between the minimum and the maximum slopes of the surface $v = m_{mn}/m_{mx}$. DeVaal [7] presents the expressions to compute the thermal constriction factor ϕ in detail.

The contact parameters a, b, n and A_r/A_a, appearing in (1) and (2), are obtained from the surface geometry and the deformation models. By assuming that the surface heights and slopes are independent and follow the Gaussian distribution, as well as assuming that the surfaces undergo plastic deformation, Cooper *et al.* [1] presented an analysis to derive expressions for the contact parameters. Yovanovich [8] presented the contact parameter expressions for the isotropic plastic model in a more convenient form. Mikic [9] extended the Cooper *et al.* [1] plastic model for the case of elastic deformation by assuming that the asperities are spherical near the tips and using results from the Hertz elastic contact theory. DeVaal [7] developed the contact parameter expressions for the contact between anisotropic surfaces under plastic deformation. The expressions for the contact parameters for all these models are shown in Table I. In this table, σ is the RMS roughness of the surface, m is the mean absolute slope of the surface and λ is the dimensionless mean separation gap between the two contact surfaces ($=Y/\sigma$). The roughness parameters σ and m can be easily obtained from roughness measurements using equipments such as stylus profilometers.

The dimensionless plastic contact pressure P/H_c appearing in (8) of Table I can be computed using the model proposed by Song and Yovanovich [10]

$$\frac{P}{H_c} = \left[\frac{P}{c_1\,(1.62\sigma/m)^{c_2}}\right]^{1/(1+0.071c_2)}. \tag{3}$$

The equivalent Young's modulus E' appearing in (9) of Table I is

$$E' = \left(\frac{1-\upsilon_A^2}{E_A} + \frac{1-\upsilon_B^2}{E_B}\right)^{-1}. \tag{4}$$

TABLE I
CONTACT PARAMETER EXPRESSIONS

Surface	*Contact Parameters*
Isotropic ref.[8,9]	$n = \frac{1}{16}\left(\frac{m}{\sigma}\right)^2 \frac{\exp\left(-\lambda^2\right)}{erfc\left(\lambda/\sqrt{2}\right)}$ (5)
	$a = \frac{2\sqrt{\kappa}}{\sqrt{\pi}}\frac{\sigma}{m}\exp\left(\frac{\lambda^2}{2}\right)erfc\left(\frac{\lambda}{\sqrt{2}}\right)$ (6)
	$\lambda = Y/\sigma = \sqrt{2}\,erfc^{-1}\left(2A_r/A_a\right)$ (7)
	$A_r/A_a = \begin{cases} P/H_c & for\ plastic \\ \sqrt{2}P/mE' & for\ elastic \end{cases}$ (8), (9)
	$\kappa = \begin{cases} 2, & for\ plastic \\ 1, & for\ elastic \end{cases}$ (10)
Anisotropic (plastic deformation only) ref. [7]	$n = \frac{1}{16}\left(\frac{m}{\sigma}\right)^2 \frac{\exp\left(-\lambda^2\right)}{erfc\left(\lambda/\sqrt{2}\right)}$ (11)
	$a = \frac{2\sqrt{2}}{\sqrt{\pi}}\frac{\sigma}{m_{mn}}\exp\left(\frac{\lambda^2}{2}\right)erfc\left(\frac{\lambda}{\sqrt{2}}\right)$ (12)
	$b = \frac{2\sqrt{2}}{\sqrt{\pi}}\frac{\sigma}{m_{mx}}\exp\left(\frac{\lambda^2}{2}\right)erfc\left(\frac{\lambda}{\sqrt{2}}\right)$ (13), (14)
	$\lambda = Y/\sigma = \sqrt{2}\,erfc^{-1}\left(2A_r/A_a\right)$ (15)
	$A_r/A_a = P/H_c$

Sridhar and Yovanovich [5] made an extensive review of the thermal contact conductance models available in the literature. Most of the models showed similar results as the models reviewed in this section. The authors also compared the models against experimental data and concluded that the models based on the Cooper *et al.* [1] model, presented in this section, are very accurate especially at high contact pressures. At light loads, the models tend to underpredict the experimental data. In the next section, it will be shown that the assumption of Gaussian asperity height distribution leads to underestimation of thermal contact conductance at light contact loads. A new model, called Truncated Gaussian model, is proposed here as the modified geometry model.

III. ACTUAL SURFACE HEIGHT DISTRIBUTIONS

The assumption of Gaussian height distribution was first analyzed in more detail by Greenwood and Williamson [2]. They measured surface roughness profiles of bead blasted aluminum surfaces and concluded that the Gaussian distribution is a good approximation at least in the range of surface heights between $\pm 2\sigma$, where σ is the RMS of the heights of the profile.

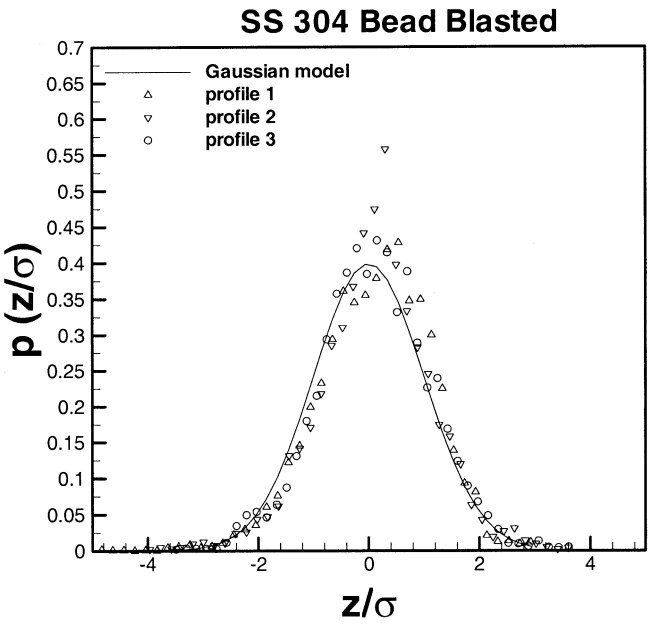

Fig. 1. Measured height distributions of three different profiles of a SS 304 bead blasted surface and comparison with the Gaussian model.

Fig. 1 shows measured surface height distributions obtained from three different profiles of a typical bead blasted SS 304 surface, obtained using commercially available bead blasting equipment and glass beads. The Gaussian model is also plotted in this graph and it is in good agreement with the measurements for surface heights in the range, especially in the range of $1.5 \leq z/\sigma \leq 3.7$. In typical engineering applications, the mean separation between the contacting surfaces lies in this range. If this surface is brought into contact with a flat lapped surface, for instance, under a contact pressure of $P/H_c = 10^{-6}$, which is a very light contact pressure, one can use (7) and (8) to calculate a mean separation gap of $Y \cong 4.7\sigma$, according to the Gaussian geometry model. However, the measured profile height distributions do not show asperities higher than 3.7σ. The profile height distributions follow the Gaussian distribution up to $z \cong 3.7\sigma$, where they are truncated. This is expected to be the maximum mean plane separation under the lightest contact load. Therefore, the Gaussian model seems to overpredict the mean plane separation under these circumstances. Since the actual mean plane separation is smaller than predicted by the Gaussian model, the actual thermal contact conductance will be larger than predicted.

Several other researchers [6], [7], [11], among others also measured profile height distributions of actual machined surfaces and concluded that the Gaussian model is a good approximation. They presented actual surface profile height measurements truncated between 3 and 4 σ, but they did not observe the truncation. Only Song [11] identified the consequences of the asperity truncation on the contact conductance problem. He studied the gap conductance problem and proposed a modified expression to compute the mean plane separation between the contacting surfaces.

This expression was derived assuming that the asperity height distribution follows the Gaussian model but is truncated at some

height level, called here λ_{trunc}. The modified expression for the mean plane separation λ_{TG} is written in the following form:

$$\lambda_{TG} = \frac{Y_{TG}}{\sigma} = \sqrt{2}\, erfc^{-1}\left[2\,\frac{A_r}{A_a} + erfc\left(\frac{\lambda_{trunc}}{\sqrt{2}}\right)\right] \quad (16)$$

where, *TG* stands for Truncated Gaussian and λ_{trunc} is the normalized height above which the Gaussian distribution is truncated. Therefore, λ_{trunc} is the height of the highest (truncated) asperities, while λ_{TG} is the separation between two surfaces in contact according to the Truncated Gaussian model. When the real-to-apparent area ratio A_r/A_a is small, that is, the contact pressure is small (approximately less than 10^{-4}), the second term between the square brackets of (16) has the same order of magnitude as A_r/A_a. That means that the truncation of the asperities is very important below this contact pressure level. As the contact pressure increases A_r/A_a becomes much larger than $erfc(\lambda_{trunc}/\sqrt{2})$, and (16) can be approximated by (7) and (14), which represent the fully Gaussian model. Physically, this means that as the pressure increases, more and more asperities come into contact, and as a consequence, the effect of the very few truncated asperities becomes negligible.

Song [11] used (16) in his gap conductance model (heat transfer through the gas filling the gaps between the contacting surfaces), compared the results against experimental data and observed good agreement. However, when he tried to use the modified mean separation gap expression [see (16)] to predict contact conductance data (conduction through the contact spots), the results of the TG model were much worse than the fully Gaussian model. The present authors now believe that Song [11] was not successful in applying the TG geometry model in the contact conductance model because he used the expression for the mean contact spot radius according to the fully Gaussian model [see (6)]. A new expression for the mean contact spot radius, according to the truncated Gaussian model, is derived in this work and presented in the next section.

IV. Truncated Gaussian Contact Conductance Model

The asperity height distributions shown in Fig. 1 were obtained from a bead blasted surface, but the authors also analyzed ground and lapped surfaces and found that the results were very similar to bead blasted surfaces: the distributions were truncated at some height level between 3 and 4 σ, approximately. These commonly employed machining processes do not generate asperities higher than this level. The reason for this is still unclear.

In the Truncated Gaussian model, it is assumed that the higher asperities are shorter than predicted by the fully Gaussian model, but they are not missing. The total number of asperities remains the same, although the highest asperities are truncated. Based on this model, the expression for the contact spot density n, (5) and (11), are still valid. The correct expression to compute the mean separation gap is now (16), instead of (7) and (14). Also, the mean contact spot radius a [see (6)] must be corrected using the following expression:

$$a_{TG} = a\sqrt{1 - \frac{erfc\left(\lambda_{trunc}/\sqrt{2}\right)}{erfc\left(\lambda_{TG}/\sqrt{2}\right)}} \quad (17)$$

where a_{TG} is the mean contact spot radius according to the Truncated Gaussian model and a is the mean contact spot radius according to fully Gaussian model [see (6)]. The expression above was obtained by solving ($n\pi a_{TG}^2 = A_r/A_a$) for a_{TG}, where A_r/A_a is obtained from (16). The expressions for the semi-major and semi-minor axes for the mean elliptical contact spot of the anisotropic plastic model, (12) and (13), become similar to the above expression. The real-to-apparent contact area ratio, the last required contact parameter is computed in the same way as before [see (7), (8), and (15)] because these expressions are obtained from force balances and do not depend on the geometric model used.

The next section presents a comparison between the TG contact conductance model and experimental data available in the literature.

V. Comparison Between TG Model and Experimental Data

Hegazy [4] collected a large quantity of thermal contact conductance data between lapped and bead blasted specimens of SS 304, Ni 200, Zr-4 and Zr-Nb possessing various roughness levels. He compared his data with the Cooper *et al.* [1] isotropic plastic model and noticed that at light contact pressures the model underpredicts the data for all the materials and roughness levels tested. He proposed an explanation for this unexpected behavior as being a consequence of thermal strain and flatness deviations of the test specimens. However, he clearly stated that this explanation was not definitive and further work was needed to clarify this phenomenon. This issue is addressed here and is explained in the light of the new Truncated Gaussian geometric model.

Figs. 2–4 show the thermal contact conductance experimental data obtained by Hegazy [4] for different metals and different roughness levels. The TG model is also plotted in these graphs as a set of curves for different truncation levels λ_{trunc} because Hegazy [4] did not provide information about the surface height distribution truncation level of his test specimens. The plots show the dimensionless thermal contact conductance C_c as a function of dimensionless contact pressure P/H_c. The dimensionless contact pressure was computed using (3), and the dimensionless contact conductance is defined as

$$C_c = \frac{h_c \sigma}{k_s\, m}. \quad (18)$$

The lowest curve of each graph is for $\lambda_{trunc} = +\infty$, which is equivalent to the fully Gaussian model. For practical purposes, a value of $\lambda_{trunc} = 5$ is sufficient for the TG model to coincide with the fully Gaussian model. The curve for the fully Gaussian model appears as a straight line in the log-log plots. The curves for the TG model for $\lambda_{trunc} < 5$ are concave: they lie above the fully Gaussian model at light contact pressures and tend to the fully Gaussian model as the contact pressure increases. The higher the truncation level (smaller λ_{trunc}), the larger the departure of the TG model from the fully Gaussian model. The TG model seems to predict the experimental data trend very well. The experimental data lie between the curve of $\lambda_{trunc} = 3.4$ and the curve of the fully Gaussian Model ($\lambda_{trunc} = +\infty$).

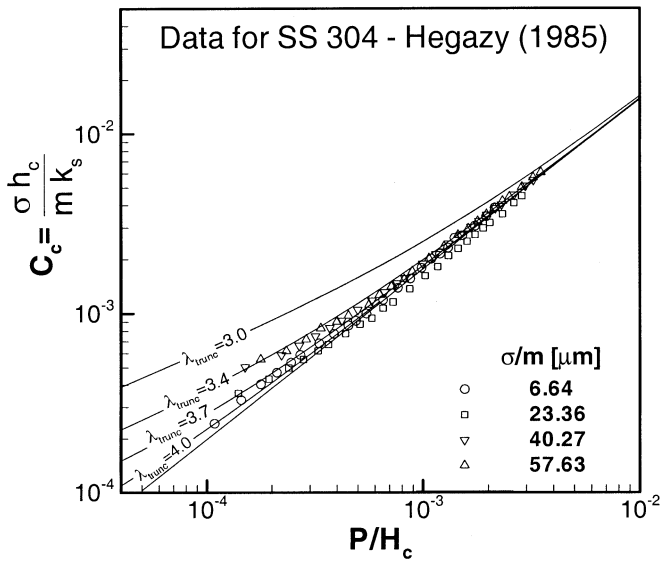

Fig. 2. Thermal contact conductance data for SS 304 from Hegazy [4] and comparison against the TG model.

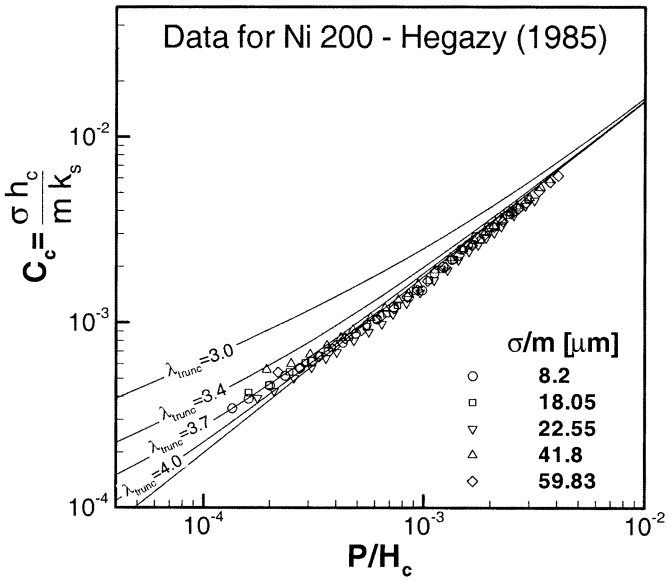

Fig. 3. Thermal contact conductance data for Ni 200 from Hegazy [4] and comparison against the TG model.

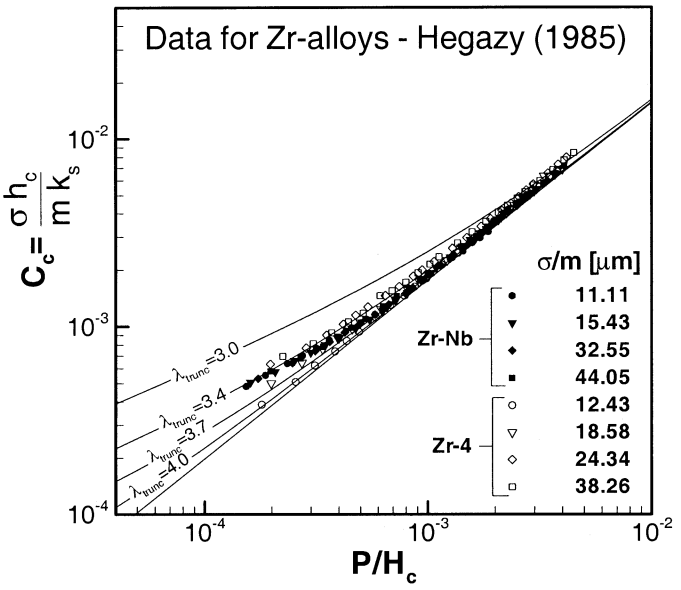

Fig. 4. Thermal contact conductance data for Zr-alloys from Hegazy [4] and comparison against the TG model.

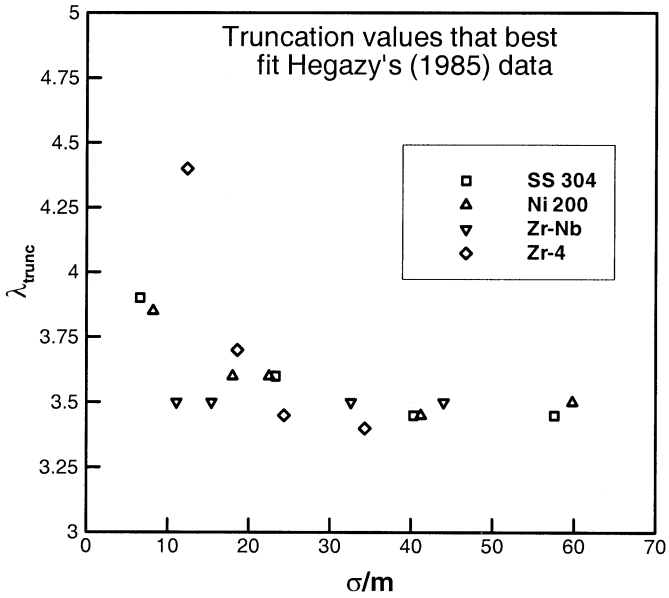

Fig. 5. λ_{trunc} values that best fit TG model to experimental data from Hegazy [4] versus σ/m.

VI. Levels of Truncation of Real Surfaces

Fig. 5 shows a graph of the values of λ_{trunc} that best fit Hegazy's [4] data as a function of σ/m. Different λ_{trunc} are observed for distinct metals possessing the same σ/m, although in general λ_{trunc} decreases with σ/m. The values of λ_{trunc} for different metals are scattered between 3.5 and 4.5 for small σ/m and tend to approximately 3.5 for large σ/m.

The above results show that it is necessary to predict λ_{trunc} for different metals and for different roughness levels. Given the difficulty in modeling analytically the bead blasting process or any other machining process, it seems very difficult to predict λ_{trunc} theoretically. Another option is to measure λ_{trunc} using a profilometer, the same equipment used to measure σ and m. Most of the profilometers available commercially measure a roughness parameter that represents the height of the highest peak of the profile, generally known as R_p [μm]. Song [11] used the R_p collected from a single profilometer trace as a measure for the truncation ($\lambda_{trunc} = R_p/\sigma$). However, it looks very unlikely that a single trace is able to pass through the peak of the highest asperity of the surface. On the other hand, if one decides to take several different profiles and one of the traces comes across an asperity much higher than the others, this single asperity could not represent the truncation level of the entire surface either because one single asperity can not support the entire contact load alone, even a very light contact load.

In an effort to better understand the truncation of real surface height distributions, the authors decided to undertake a more detailed study of the surface generation process. The authors chose the bead blasting process for this study for various reasons. One

can start from a flat lapped surface and by bombarding the surface with glass beads at high speeds, one can "grow" the asperities on the surface at practically any desired RMS roughness level (R_q).

Several bead blasting parameters, such as bead size, air pressure and exposure time can be adjusted in order to generate the desired roughness level. Moreover, this process has been applied very successfully by other thermal contact resistance researchers [3], [4], [6], [11], among others to generate randomly distributed asperities on the surface without affecting its flatness, which is very important in order to guarantee that the surface geometry is in accordance with the geometric model.

Truncation of Bead Blasted Surfaces

The bead blasting study consisted of measuring the roughness parameters R_p (maximum profile height), σ (profile height RMS) and m (profile mean absolute slope) as well as the general trend of the asperity height distribution as a function of bead blasting exposure time between 1 and 16 min. Three different blasting pressures (10, 20, and 40 ps) and three different glass bead size ranges (125–180 μm, 279–420 μm and 590–840 μm) were used. Four profiles were assessed over each generated surface, resulting in a total of 136 profile measurements. The minimum and maximum σ/mratios measured during the tests were 12 and 44 μm, respectively. The first important conclusion from this study was that the general trend of the surface height distribution was Gaussian independent of the blasting parameter combinations analyzed. Both the profile height RMS (σ) and mean absolute slope (m) as well the ratio σ/m increase with increasing exposure time and blasting pressure, as expected, especially for the smaller glass beads. For the largest bead size range tested, the exposure time did not significantly affect either σ or m. The blasting pressure was found to be the most important parameter in determining the roughness level.

The main goal of the bead blasting study was to analyze the truncation levels of the surface height distributions for every combination of blasting parameters. It was found that the measured R_p/σ (normalized maximum profile height) presented very different values for different profiles collected from the same surface. The largest R_p/σ difference measured from different profiles on a single surface was more than 100%. The variation between R_p/σ values measured on the same surface was much larger than the variation between the mean values of R_p/σ from different surfaces. Also, the average of the four R_p/σ readings on each surface varied randomly among different surfaces. In other words, the R_p/σ ratio seemed not to be controlled by any of the bead blasting parameters.

The authors then decided to verify whether the measured R_p/σ values could be related to the roughness level of the surface, as observed from the comparison between the TG model and the experimental data [4], independent of the blasting parameters employed. Fig. 6 shows a plot of all 136 measured R_p/σ values as a function of σ/m for all combinations of blasting parameters analyzed. The R_p/σ values lie in a large band, which seems to become narrower as σ/m increases. The mean value of R_p/σ also seems to experience a slight decrease with increasing σ/m. These observations are in accordance with the previous conclusion from the comparison between the

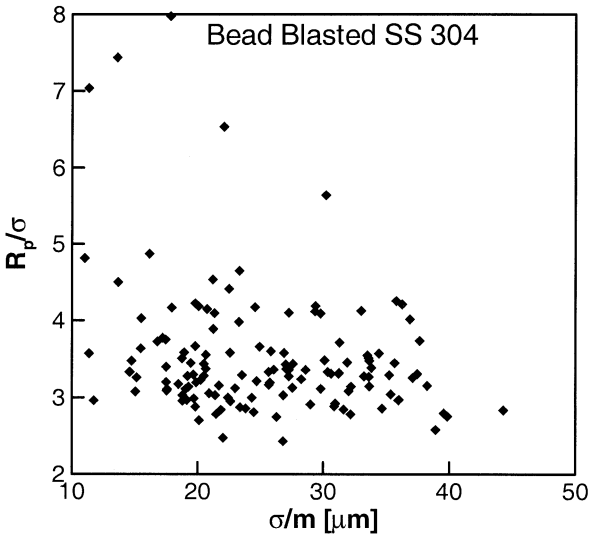

Fig. 6. R_p/σ versus σ/m for bead blasted SS 304 surfaces.

TG model and the thermal data from Hegazy [4] that λ_{trunc} decreases with increasing σ/m (Fig. 5). Also, the observation from the thermal tests that λ_{trunc} is larger than 3.5 also is consistent with the R_p/σ measurements presented in Fig. 6.

The question of how to predict λ_{trunc} from roughness measurements still remains unanswered. However, it is clear that a single profile measurement is not sufficiently accurate to measure λ_{trunc} because there are only a few truncated asperities and the probability of a single profile trace capture at least one of the truncated asperities is very small. As it can be see from Figs. –4, the TG model is very sensitive to the value of λ_{trunc}, and the measured R_p/σ present large variations for the same surface. The authors believe that the best way to obtain information on the correct truncation level is from thermal contact conductance experiments.

Similar to the method used to obtain the values presented in Fig. 5, by inputting the λ_{trunc} value that best fits the TG contact conductance model to the experimental data one can extract information on λ_{trunc}. Therefore, more thermal contact conductance data need to be generated for this purpose, especially in the light contact pressure range.

VII. Conclusion

The observation that the existing thermal contact conductance models underpredict experimental data at light contact pressures is reported in several previous thermal contact conductance studies. This work presents evidence that the well-accepted Gaussian surface height distribution geometry model causes the thermal contact conductance models to underpredict the experimental data at light contact pressures. Surface height distribution measurements show that although the distributions follow the Gaussian model for surface heights larger than 1.5 σ, the distributions are truncated generally between 3 and 4 σ. A new thermal contact conductance model is proposed based on the Truncated Gaussian geometry model. The preliminary results show that the new model predicts the data trend very well. The new model requires another surface parameter, called λ_{trunc}, in addition to the parameters σ and m. It is not clear at

this point how to obtain this third surface parameter from profilometer traces. The use of thermal contact conductance data seems to be the best way to obtain this information.

The truncation of the surface height distribution and its effects on the thermal contact conductance problem is a very important finding but also very recent. Additional studies are needed in order to clarify the questions raised here, especially regarding to the prediction and/or the control of the truncation level of actual machined surfaces.

REFERENCES

[1] M. Cooper, B. Mikic, and M. M. Yovanovich, "Thermal contact conductance," *J. Heat Mass Transfer*, vol. 12, pp. 279–300, 1969.

[2] J. A. Greenwood and J. B. P. Williamson, "Contact of nominally flat surfaces," in *Proc. Royal Soc. London*, 1966, pp. 300–319.

[3] F. H. Milanez, J. R. Culham, and M. M. Yovanovich, "Experimental study on the hysteresis effect of thermal contact conductance at light loads," in *Proc. 40th AIAA Aerosp. Sci. Meeting Exhibit*, Reno, NV, Jan. 14–17, 2002, AIAA-2002-0787.

[4] A. A. Hegazy, "Thermal joint conductance of conforming rough surfaces: Effect of surface micro-hardness variation," Ph.D. dissertation, Univ. of Waterloo, Waterloo, ON, Canada, 1985.

[5] M. R. Sridhar and M. M. Yovanovich, "Thermal contact conductance of tool steel and comparison with model," *Int. J. Heat Mass Transfer*, vol. 39, no. 4, pp. 831–839, 1996.

[6] K. M. Nho, "Experimental investigation of heat flow rate and directional effect on contact conductance of anisotropic ground/lapped interfaces," Ph.D. dissertation, Univ. of Waterloo, Waterloo, ON, Canada, 1990.

[7] J. W. DeVaal, "Thermal joint conductance of surfaces prepared by grinding," Ph.D. dissertation, University of Waterloo, Ontario, 1988.

[8] M. M. Yovanovich, "Thermal contact correlations," in *Spacecraft Radiative Heat Transfer and Temperature Control*, T. E. Horton, Ed. New York: Progress in Astronautics and Aeronautics, 1981, vol. 83.

[9] B. B. Mikic, "Thermal contact conductance; Theoretical considerations," in *J. Heat Mass Transfer*. New York: Pergamon, 1974, vol. 17, pp. 205–214.

[10] S. Song and M. M. Yovanovich, "Relative contact pressure: Dependence on surface roughness and Vickers microhardness," *J. Thermophys. Heat Transfer*, vol. 2, no. 4, pp. 633–640, 1988.

[11] S. Song, "Analytical and experimental study of heat transfer through gas layers of contact interfaces," Ph.D. dissertation, Univ. of Waterloo, Waterloo, ON, 1988.

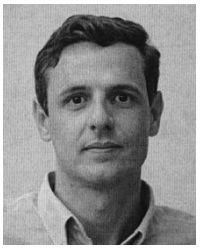

Fernando H. Milanez received the B.S. and M.S. degrees in mechanical engineering from the Federal University of Santa Catarina, Brazil, in 1996 and 1999, respectively, and is currently pursuing the Ph.D. degree in thermal contact conductance at the University of Waterloo, Waterloo, ON, Canada.

He is with the Satellite Thermal Control Group, University of Waterloo. He has been also working on the development of thermal control devices for space applications and his field of interests are thermodynamics, heat transfer, and transport phenomena.

M. Michael Yovanovich is a Distinguished Professor Emiritus of mechanical engineering at the University of Waterloo, Waterloo, ON, Canada, and is the Principal Scientific Advisor to the Microelectronics Heat Transfer Laboratory. His research in the field of thermal modeling includes analysis of complex heat conduction problems, natural and forced convection heat transfer from complex geometries, and contact resistance theory and applications. He has published more than 300 journal and conference papers and numerous technical reports. He has been a consultant to several North American nuclear, aerospace, and microelectronics industries and national laboratories.

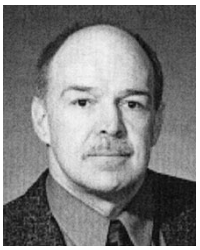

J. Richard Culham (M'98) is an Associate Professor of mechanical engineering at the University of Waterloo, Waterloo, ON, Canada. He is the Director and a Founding Member of the Microelectronics Heat Transfer Laboratory. Research interests include modeling and characterization of contacting interfaces and thermal interface materials, development of compact analytical and empirical models at micro- and nano-scales, natural and forced convection cooling, optimization of electronics systems using entropy generation minimization, and the characterization of thermophysical properties in electronics materials. He has more than 80 publications in refereed journals and conferences in addition to numerous technical reports related to microelectronics cooling.

Dr. Culham is a member of ASME and the Professional Engineers Association of Ontario.